

ARTICLES

 p_t and x_F dependence of the polarization of Σ^+ hyperons produced by 800 GeV/c protons

A. Morelos,^{1,*} I. F. Albuquerque,^{6,†} N. F. Bondar,³ R. Carrigan, Jr.,¹ D. Chen,^{10,‡} P. S. Cooper,¹ Dai Lisheng,² A. S. Denisov,³ A. V. Dobrovolsky,³ T. Dubbs,^{5,§} A. M. F. Endler,⁸ C. O. Escobar,⁶ M. Foucher,^{7,||} V. L. Golovtsov,³ H. Gottschalk,^{1,¶} P. Gouffon,⁶ V. T. Grachev,³ A. V. Khazadzev,³ M. A. Kubantsev,⁴ N. P. Kuropatkin,³ J. Lach,¹ Lang Pengfei,² V. N. Lebedenko,⁴ Li Chengze,² Li Yunshan,² M. Luksys,¹³ J. R. P. Mahon,^{6,**} E. McCliment,⁵ C. Newsom,⁵ M. C. Pommot Maia,^{9,††} V. M. Samsonov,³ V. A. Schegelsky,³ Shi Huanzhang,² V. J. Smith,¹¹ Tang Fukun,² N. K. Terentyev,³ S. Timm,^{12,‡‡} I. I. Tkatch,³ L. N. Uvarov,³ A. A. Vorobyov,³ Yan Jie,² Zhao Wenheng,² Zheng Shuchen,² and Zhong Yuanyuan²

(E761 Collaboration)

¹Fermi National Accelerator Laboratory, Batavia, Illinois 60510

²Institute of High Energy Physics, Beijing, People's Republic of China

³St. Petersburg Nuclear Physics Institute, Gatchina, Russia

⁴Institute of Theoretical and Experimental Physics, Moscow, Russia

⁵University of Iowa, Iowa City, Iowa 52242

⁶Universidade de Sao Paulo, Sao Paulo, Brazil

⁷J. W. Gibbs Laboratory, Yale University, New Haven, Connecticut 06511

⁸Centro Brasileiro de Pesquisas Fisicas, Rio de Janeiro, Brazil

⁹Conselho Nacional de Pesquisas CNPq, Rio de Janeiro, Brazil

¹⁰State University of New York at Albany, Albany, New York 12222

¹¹H. H. Wills Physics Laboratory, University of Bristol, United Kingdom

¹²Carnegie Mellon University, Pittsburgh, Pennsylvania 15213

¹³Universidade Federal da Paraiba, Paraiba, Brazil

(Received 8 November 1993)

We utilize the angle and momentum resolution of our apparatus to study the polarization of 375 GeV/c Σ^+ hyperons produced by 800 GeV/c protons incident on a Cu target. By examining in detail two of our high statistics data samples, we find evidence for structure in the p_t dependence of Σ^+ polarization and are able to extract the x_F dependence of the Σ^+ polarization and compare it with x_F behavior in the Λ^0 and Ξ^- systems.

PACS number(s): 13.88.+e, 13.85.Ni, 14.20.Jn

Information on the kinematical dependence of polarization is an important test of theoretical hyperon production models. In this article we extract new information available in the high statistics data samples which formed the basis of a previous Letter [1]. Studying the dependence of the polarization within each data sample

yields new information on the detailed structure of the p_t and x_F dependence of the polarization of inclusively produced Σ^+ hyperons.

Although each of the data samples corresponds to only one setting of the E761 spectrometer, each includes data in a finite range of p_t and x_F corresponding to the angular and momentum acceptance of the hyperon channel [2] and spectrometer. The resolution and acceptance of the hyperon spectrometer in x_F are $\sigma(x_F)/x_F = 0.7\%$ and $\Delta x_F/x_F = \pm 8\%$ [full width at half maximum (FWHM)], respectively. In the p_t variable the spectrometer resolution and acceptance are functions of p_t . Typical values are $\sigma(p_t)/p_t = 1\%$ and $\Delta p_t/p_t = \pm 10\%$ (FWHM), respectively. For samples containing a large number of events, we have the resolution and sensitivity to extract information on the p_t and x_F dependence of the Σ^+ polarization within that data sample.

The horizontal (H) targeting angle data [1] at ± 3.7 mrad include over twelve million events and were used to measure the asymmetry parameter [3] in the $\Sigma^+ \rightarrow p\gamma$ radiative decay. Vertical (V) targeting angle data at ± 2.9 mrad containing about a quarter of a million events were taken as part of a measurement of the Σ^+ magnetic mo-

*Present address: Instituto de Fisica Universidad Autonoma de San Luis Potosi, S.L.P. 78240, Mexico.

†Present address: Department of Physics, Rutgers University, Piscataway, NJ 08855.

‡Now at Fermilab.

§Present address: Department of Physics, University of California (Santa Cruz), Santa Cruz, CA 95046.

||Present address: Department of Physics, University of Maryland, College Park, MD 20742.

¶Present address: COPPE, Universidade Federal do Rio de Janeiro, Brazil.

**Present address: Universidade Federal do Rio de Janeiro, Brazil.

††Present address: Department of Physics, Stanford University, Stanford, CA 94309.

‡‡Present address: Department of Physics, SUNY at Albany, Albany, NY 12222.

ment [4]. Our analysis rests on our understanding of the acceptance of our spectrometer to incident Σ^+ in the full range of our beam phase space. Comparing the polarizations at two nominally equal and opposite targeting angles allows us to measure the mean polarization with well controlled precision. The details of our polarization analysis algorithm are described elsewhere [5]. However, the beam phase space distributions are not identical for these two complementary angles and if we divide the events of a particular spectrometer setting into bins of equal p_t or x_F we must take this into account.

The 3.7 mrad horizontal sample and the vertical targeting sample were divided into seven and six bins in p_t , respectively. The Σ^+ polarization was computed for each of the bins and is shown in Table I and displayed in Fig. 1 with the other E761 Σ^+ polarization data [1,6]. Table I displays both the statistical and systematic uncertainty of the polarization for these points. Note that the statistical uncertainty of the polarization depends not just on the total number of events in the data bin but also on how they are divided between the two complementary targeting angles. The mean values of x_F (p_t) for the two targeting angles are shown in Table I (II). These indicate the differences in the beam phase space when the targeting angle is reversed. Our analysis technique yields the arithmetic average of the polarization of the two targeting angles: viz., $P(p_t) = \frac{1}{2}[P(x_{F+}, p_t) + P(x_{F-}, p_t)]$.

In the analysis of Ref. [1] all events were subjected to a restriction that the proton be well away from the walls of the photon calorimeter hole. Figure 2(a) of Ref. [1] shows the event mass distribution with this selection imposed. The number of events and range of p_t coverage in the vertical targeting sample can be increased significantly if we relax this restriction. The vertical targeting sample without this criterion is shown in Tables I and II. All horizontal data points retain this cut.

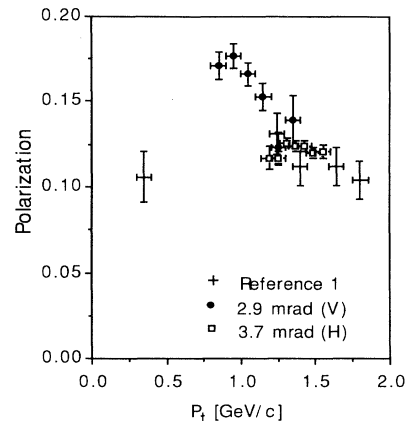


FIG. 1. Polarization for Σ^+ as a function of p_t from this experiment.

The systematic uncertainties are estimated from variations of our selection criteria in decay angle, decay vertex position, and missing mass. For the vertical targeting sample, releasing the calorimeter edge restriction increases the p_t coverage significantly; however, this also increases the mean polarization by 0.0090 ± 0.0045 , where the error is our estimate of the systematic uncertainty. This value is used to correct all bins of the vertical targeting sample. This and the other systematic uncertainties were combined in quadrature and are also given in Table I and Fig. 1. An overall scale uncertainty due to the error [7] in the determination of the α parameter of 1.6% is not included.

In Fig. 1 we note that from the vertical targeting sample alone the polarization reaches a maximum near $p_t = 1$ GeV/c. The inclusion of the 3.7 mrad sample data points confirms that the polarization has decreased by $\sim 25\%$

TABLE I. Polarization in bins of p_t . The values of x_F of positive and negative targeting angles are shown as x_{F+} and x_{F-} , respectively. The polarization errors are statistical and systematic, respectively. The vertical targeting sample polarizations are corrected as noted in the text.

Angle (mrad)	Events	x_{F+}	x_{F-}	$\langle p_t \rangle$ (GeV/c)	Polarization
0.9 H	14 134	0.463	0.483	0.35	$0.106 \pm 0.015 \pm 0.003$
2.9 V	86 480	0.445	0.445	0.85	$0.171 \pm 0.006 \pm 0.006$
2.9 V	237 087	0.455	0.455	0.95	$0.177 \pm 0.004 \pm 0.006$
2.9 V	204 625	0.465	0.465	1.05	$0.166 \pm 0.004 \pm 0.006$
2.9 V	136 187	0.475	0.475	1.15	$0.153 \pm 0.005 \pm 0.006$
2.9 V	69 990	0.485	0.485	1.25	$0.123 \pm 0.007 \pm 0.006$
2.9 V	14 684	0.495	0.495	1.35	$0.139 \pm 0.014 \pm 0.006$
3.3 H	20 351	0.463	0.483	1.24	$0.131 \pm 0.012 \pm 0.003$
3.7 H	227 055	0.442	0.518	1.19	$0.117 \pm 0.006 \pm 0.003$
3.7 H	808 435	0.448	0.508	1.25	$0.117 \pm 0.002 \pm 0.003$
3.7 H	2 013 063	0.456	0.496	1.31	$0.126 \pm 0.001 \pm 0.003$
3.7 H	2 962 453	0.461	0.488	1.37	$0.124 \pm 0.001 \pm 0.003$
3.7 H	2 785 141	0.467	0.478	1.43	$0.124 \pm 0.001 \pm 0.003$
3.7 H	1 813 897	0.473	0.468	1.49	$0.120 \pm 0.001 \pm 0.003$
3.7 H	946 869	0.479	0.457	1.55	$0.121 \pm 0.002 \pm 0.003$
3.8 H	43 225	0.463	0.483	1.40	$0.112 \pm 0.011 \pm 0.003$
4.3 H	23 173	0.463	0.483	1.64	$0.112 \pm 0.011 \pm 0.003$
4.8 H	23 744	0.463	0.483	1.80	$0.104 \pm 0.011 \pm 0.003$

TABLE II. Polarization in bins of x_F . The values of p_t of positive and negative targeting angles are shown as p_{t+} , and p_{t-} , respectively. The polarization errors are statistical and systematic, respectively. The vertical targeting sample polarizations are corrected as noted in the text.

Angle (mrad)	Events	P_{t+} (GeV/c)	P_{t-} (GeV/c)	x_F	Polarization
2.9 V	5 087	1.02	1.02	0.445	$0.116 \pm 0.026 \pm 0.003$
2.9 V	38 077	1.04	1.04	0.455	$0.147 \pm 0.010 \pm 0.003$
2.9 V	79 080	1.07	1.07	0.465	$0.157 \pm 0.007 \pm 0.003$
2.9 V	77 284	1.09	1.09	0.475	$0.169 \pm 0.007 \pm 0.003$
2.9 V	40 579	1.11	1.11	0.485	$0.171 \pm 0.009 \pm 0.003$
2.9 V	9 174	1.13	1.13	0.495	$0.199 \pm 0.020 \pm 0.003$
3.7 H	1 206 016	1.33	1.46	0.455	$0.125 \pm 0.002 \pm 0.003$
3.7 H	1 872 136	1.37	1.45	0.461	$0.119 \pm 0.002 \pm 0.003$
3.7 H	2 249 978	1.41	1.43	0.467	$0.118 \pm 0.001 \pm 0.003$
3.7 H	2 166 507	1.45	1.42	0.473	$0.126 \pm 0.001 \pm 0.003$
3.7 H	1 773 641	1.49	1.40	0.479	$0.122 \pm 0.001 \pm 0.003$
3.7 H	1 278 412	1.53	1.39	0.485	$0.128 \pm 0.002 \pm 0.003$
3.7 H	811 293	1.57	1.37	0.491	$0.136 \pm 0.003 \pm 0.003$

from $p_t = 1.0$ to $p_t = 1.4$ GeV/c and the rate of decrease has become less. QCD predicts [7] that the polarization should vanish at large p_t and rotational invariance requires that it be zero at $p_t = 0$. However, vanishing at zero and large p_t does not preclude complex behavior in intermediate p_t regions.

We choose to divide the event samples in these two high statistics samples in equal bins of x_F and study the x_F dependence of Σ^+ polarization for two different

values of p_t . This is shown in Table II and displayed in Fig. 2(a) for each of these samples. In each case we see the polarization increasing with x_F . These distributions have been fitted to a straight line whose slope (dp/dx_F) indicates the change of polarization as a function of x_F . The fitted values of dp/dx_F are given in Table III.

In order to attempt an understanding of the polarization mechanism, comparison with other hyperons is important. Hyperon production polarization data with 400 GeV incident protons exist in a similar kinematical region for the Λ^0 system [9]. Even though these data extend out to much larger values of p_t , they do not show a falloff similar to that of the Σ^+ polarization. The model of hyperon polarization increasing linearly with p_t until $p_t \approx 1$ GeV/c and then becoming constant [10] is not an adequate description of the Σ^+ data presented here.

Data at 800 GeV are available for the Ξ^- system [10]. Both the Ξ^- and Λ^0 measurements use a Be target as contrasted to the Cu target used by us. From these two studies we can select data in a similar region of p_t and compare the x_F dependence to our Σ^+ measurements. These are plotted in Figs. 2(b) and 2(c). The fitted slopes are given in Table III. The effect of target materials has only been studied for the Λ^0 system. In these studies target effects [11] were seen to be small. We assume that this is true for the other hyperons as well.

The plots of Fig. 2 show the differing behavior of the x_F dependence of the polarization for Σ^+ , Λ^0 , and Ξ^- at two different values of p_t . In looking at the Σ^+ and Λ^0 plots one first notices that the signs of the polarizations are opposite. All models which incorporate the constituent quark picture are in agreement with this fact and also with the sign of the Ξ^- polarization. Taking into account the differing sign of the Σ^+ and Λ^0 polarizations, we see that their slopes dp/dx_F are of equal magnitude. In contrast, the Ξ^- polarization is independent of x_F . In the constituent quark picture the Σ^+ and Λ^0 may contain two of the three incident proton quarks whereas in the Ξ^- case at most one of the proton quarks may be incorporated into the hyperon. This suggests that the mechanisms for producing the polarization may

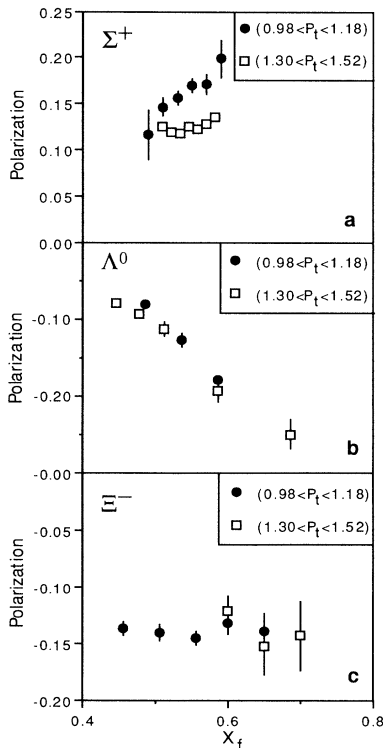


FIG. 2. Polarization of (a) Σ^+ , this work, (b) Λ^0 , Ref. [8], and (c) Ξ^- , Ref. [9], as a function of x_F for two values of p_t .

TABLE III. Polarization x_F slopes.

Particle	Energy (GeV)	Ref.	Target	dp/dx_F	
				$0.98 < p_t < 1.18$	$1.30 < p_t < 1.52$
Σ^+	800	This work	Cu	1.11 ± 0.36	0.31 ± 0.12
Λ^0	400	[9]	Be	-0.66 ± 0.07	-0.48 ± 0.04
Ξ^-	800	[10]	Be	-0.01 ± 0.06	-0.40 ± 0.27

be very different. This hypothesis is supported by the observation of antihyperon polarization [1,12], where no constituent quarks are shared with the incident proton.

There is now a growing body of experimental data on hyperon inclusive polarization. In comparing the kinematical and particle dependence of hyperon polarization, we may gain insight into the underlying mechanisms responsible for the polarization. Why does the Σ^+ polarization magnitude decrease beyond $p_t \sim 1.0$ GeV/ c whereas the Λ^0 does not? Is there something unique about the Σ^+ ? The magnitudes of the x_F dependence of hyperon polarization are similar for Σ^+ and Λ^0 . Is the fact that they differ from the Ξ^- dependence just a reflection of the number of quarks transferred from the projectile to the hyperon? How are we to account for antihyperon polarization and the different energy dependencies of Σ^+ and Ξ^- polarizations [1,12]? The only clear conclusion left in this field is that there are many more questions than answers.

We wish to thank the staffs of Fermilab and the Petersburg Nuclear Physics Institute for their assistance. The loan of the photon calorimeter lead glass from Rutgers University is gratefully acknowledged. The BGO crystals were produced by the Shanghai Institute of Ceramics, Academia Sinica, Shanghai, People's Republic of China. This work was supported in part by the U.S. Department of Energy under Contracts No. DE-AC02-76CH03000, No. DE-AC02-76ER03075, and Grants No. DE-FG02-91ER40682, No. DE-FG02-91ER40664, and No. DE-FG02-91ER40631, the Russian Academy of Sciences, the Chinese National Natural Science Fund (DE-19075049 and DE-19375041), and the U.K. Science and Engineering Research Council. I.F.A. was supported by FAPESP, Brazil. P.G. and J.R.P.M. were partially supported by FAPESP and CNPq, Brazil. A.M. was partially supported by CONACyT, Mexico. M.A.K. was partially supported by the International Science Foundation.

- [1] A. Morelos *et al.*, Phys. Rev. Lett. **71**, 2172 (1993).
 [2] T. R. Cardello *et al.*, Phys. Rev. **32**, 1 (1985).
 [3] M. Foucher *et al.*, Phys. Rev. Lett. **68**, 3004 (1992).
 [4] A. Morelos *et al.*, Phys. Rev. Lett. **71**, 3417 (1993).
 [5] S. Timm *et al.*, Phys. Rev. D **51**, 4638 (1995).
 [6] A. Morelos, Ph.D. thesis, Centro de Investigacion y de Estudios Avanzados del IPN, Mexico, 1992.

- [7] Particle Data Group, K. Hikasa *et al.*, Phys. Rev. D **45**, S1 (1992).
 [8] G. L. Kane *et al.*, Phys. Rev. Lett. **41**, 1689 (1978).
 [9] B. Lundberg *et al.*, Phys. Rev. D **40**, 3557 (1989).
 [10] J. Duryea *et al.*, Phys. Rev. Lett. **67**, 1193 (1991).
 [11] L. Pondrom, Phys. Rep. **122**, 57 (1985).
 [12] P. M. Ho *et al.*, Phys. Rev. Lett. **65**, 1713 (1990).